Materials Science

http://www.aimspress.com/journal/Materials

AIMS Materials Science, 5(4): 699–710.
DOI: 10.3934/matersci.2018.4.699
Received: 09 June 2018
Accepted: 06 August 2018
Published: 14 August 2018

Research article

Influence of TiC addition on the surface roughness during turning of AA 7075 alloy processed through stir-casting

Subbarayan Sivasankaran*

Department of Mechanical Engineering, College of Engineering, Qassim University, Buraidah-51452, Saudi Arabia

* **Correspondence:** Email: sivasankarangs1979@gmail.com, s.udayar@qu.edu.sa; Tel: +966534810975.

Abstract: This research work had focused on manufacturing AA 7075/(0, 2.5, 5 and 7.5 wt%) TiC metal matrix composites through stir casting route. The manufactured composites had effectively characterized using the optical microscope. It had observed from the optical microstructures that the uniform distribution of TiC ceramic particles and its embedding over the ductile AA 7075 matrix had successfully obtained which exhibited excellent mechanical (218 HRC for 7.5 wt% TiC composite) and machining behavior with the function of TiC particles when compared to monolithic AA 7075 alloy. There had a grain refinement in the composites due to TiC particles addition. The machinability of experiments had conducted by varying the cutting speed, the feed rate, the depth of cut and the tool nose radius. The surface roughness had measured and the results had indicated that AA 7075–7.5 wt% TiC ex-situ composites had exhibited a lower value of surface roughness which had expected to high-strength in the matrix that produced immediate shearing action when compared to other samples. Further, the tool nose radius had played a major role in the surface roughness in which higher value of tool nose radius (0.8 mm) sample had shown improved surface finish.

Keywords: AA 7075 Al alloy; TiC; metal matrix composite; characterization; mechanical properties; turning

1. Introduction

Possessing of high strength and high toughness are the major demand for all kind of lightweight materials nowadays and hence, the light-weight based, like Al-based metal matrix composites are inevitable to use [1–4]. The improved properties such as high hardness, Young's modulus, and high creep resistance can be achieved by incorporating the ceramic particles in the lightweight metal matrix [5–7]. In general, the lightweight based metallic materials are usually having lower value in strength which diminishes its applications. However, the ductile metallic materials are having the higher value of toughness. Therefore, the applications of metal matrix composites can be used nowadays in all the manufacturing industries for having both the strength and toughness [8,9]. Several metal matrix composites (MMCs) are available such as aluminium-based MMCs, copper-based MMCs, magnesium-based MMCs, titanium-based MMC's, and nickel based MMC's [10,11]. However, the aluminium matrix composites (AMCs) are extensively used in automotive, aircraft, and aerospace applications, namely, structural members, brake rotors and cylinders, fuel systems [12,13]. The main reason behind of this was due to that these AMC's have more attractive in high strength-to-weight ratio, high stiffness-to-weight ratio, high wear resistance, less cost, easily available one, more in thermal conductivity, good in thermal stability, and so on [14–16]. Several researchers have focused on and studied the Al-based MMCs reinforced with Al_2O_3, SiC, B_4C, TiB_2, ZrB_2, and TiC [17–20]. Among the various second phase particles, titanium carbide (TiC) ceramic particles are having the lower value of density, more in strength, excellent wettability with molten Al alloys, and poor in chemical reactivity with the matrix [7,9,13]. Further, AA 7075 alloy has the characteristics of easy to manufacture, good abrasive resistance, excellent corrosion resistance, good in wear resistance, higher in strength, and heat treatable alloy. Some of the applications of AA 7075 Al alloy are ships and submarines, aircraft and space crafts, trucks and rail vehicles, automobiles and prosthetic devices. In general, the MMCs/AMCs can be manufactured by various routes, namely, the powder metallurgy, the stir casting, the mechanical alloying, the diffusion bonding, the friction stir processing, the laser cladding, the squeeze casting, the physical vapour deposition, the infiltration techniques, the spray deposition, etc. [21]. Among the various routes, the stir casting process has preferred due to its simplicity, mass production, low cost, ease of applicability and flexibility.

All kind of critical mechanical parts such as the cutting tools, vehicles parts, aircraft parts, and spacecraft parts are usually produced through the turning process which is a secondary shaping process [22–24]. During the turning of any materials, the quality of turned surfaces, fatigue strength, and wear resistance are mainly influenced by the value of surface roughness [24–27]. Therefore, more attentions have given to the value of the surface roughness recently during the manufacturing of many parts through the secondary shaping process. The value of surface roughness has mainly depended on the selection of various process parameters such as the cutting speed, the feed rate, the depth of cut, and the tool nose radius. However, there is no much research work related to the turning behavior of AA 7075 alloy reinforced with TiC particles. The main aim of this research work had focused to synthesis the AA 7075–x wt% TiC composites (x = 0, 2.5, 5 & 7.5 wt%) through ex-situ stir casting technique, characterizing the fabricated composites using the optical microscope, and measuring of the surface roughness by varying different cutting parameters during CNC turning process.

2. Materials and method

2.1. Synthesis of AA 7075–TiC composites

Figure 1a shows the schematic of the stir-casting process which illustrates the addition of TiC particles into the molten matrix. Here, AA 7075 alloy matrix reinforced with the different weight percentage of TiC particles (0, 2.5, 5 & 7.5 wt%) had manufactured via the stir-casting process. Figure 1b shows the actual stir casting set-up used in the present research work. Table 1 shows the chemical composition of AA 7075 matrix alloy. Here, first, the AA 7075 alloy matrix had put in a graphite crucible, placed in the stir casting furnace, and heated to a temperature of around 800 °C. Once, the alloy had reached in a molten stage, the degasifying tablet had added in the melt by which all the unwanted slag had floated over the melt which had then be removed. Meantime, the purchased TiC ceramic particles (average particle size, <5 μm, almost spherical) had pre-heated at a temperature of 200 °C inside the pre-heater which had attached in the furnace (Figure 1b). Now, the molten matrix had stirred by means of mechanical stirrer coated with a high temperature non-stick ceramic element. The stirrer blade had made up of austenitic stainless steel and operated at 300 rpm due to which the matrix had attained vortex form. Then, the pre-heated TiC particles had mixed evenly in the matrix with the help of stirrer. It was maintained the constant speed of stirrer during mixing. The composite melt vortex had kept constant for 30 min for attaining the uniform dispersion of TiC particles with the AA 7075 matrix. The weight fraction of TiC particles had varied from 2.5 to 7.5 with the step size of 2.5. Maximum of 7.5 wt% TiC particles had mixed with the matrix due to retaining the ductility, and fluidity in addition to the strength. Finally, the melted composite had poured in a permanent metallic mold (coated with semi-solid graphite lubricants) of 30 mm in diameter with 250 mm in length. This process of manufacturing the composite casting is called as ex-situ method.

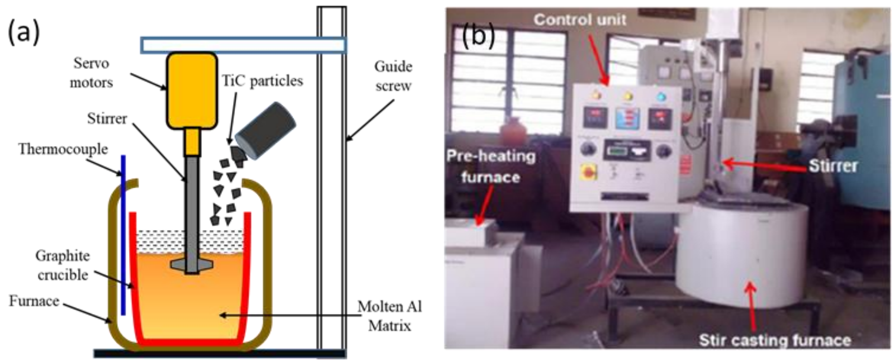

Figure 1. (a) Schematic of the stir-casting process; (b) macrograph of stir casting furnace used in the present research work.

Table 1. Chemical composition of AA 7075 alloy.

Elements	Si	Fe	Cu	Mg	Zn	Ti	Cr	Al
wt%	0.2	0.23	1.71	2.46	5.29	0.54	0.21	Bal.

2.2. Sample preparation for optical microscope and hardness test

The standard metallographic procedure had used to characterize the manufactured ex-situ AMCs samples. The small specimen size of around 10 mm diameter with 10 mm height had cold mounted using acrylic resin, polished with different SiC grit papers (400, 700, 1000, 2000, 3000 & 4000 grits/inch^2), disc polished with 9 μm alumina, and lapped using 1 μm diamond suspension. Then, the samples had chemically micro-etched using Keller's reagent (95 mL distilled water, 2.5 mL HNO_3, 1.5 mL HCL, and 1.0 mL HF). The optical microscope of Olympus BX51M had used for effective characterization. To check the bonding between the TiC particles and the matrix, SEM with EDS investigation on AA 7075–5 wt% TiC composite as an example had carried out. The mechanical behavior of the fabricated composites had checked by Rockwell hardness tester. During hardness testing, a load of 150 kgf had applied for the dwell time of 20 s. The hardness test had conducted at least ten different places and the average had used for the investigation. Before hardness testing, the samples had cleaned using acetone and then polished up to 1000 SiC grit/inch^2 sheet.

2.3. Turning experiments and surface roughness measurement

The turning experiments had carried out on Smart Jr CNC turning centre using TiN coated carbide insert (Figure 2a). The cutting speed had selected in a range of 180 to 240 mm/min, feed rate range had selected in the range of 0.1 to 0.3 mm/rev, depth of cut had selected in a range of 0.5 to 1.5 mm, and the tool insert radius of 0.4 mm and 0.8 mm had used. The Handy Surf E-DTS5706 had used to measure the surface roughness (Ra) (Figure 2b). It had consisted of a probe which recorded the surface roughness with measuring the force of 4 mN and radius diamond end of 5 µm, cone measuring probe of 90 °.

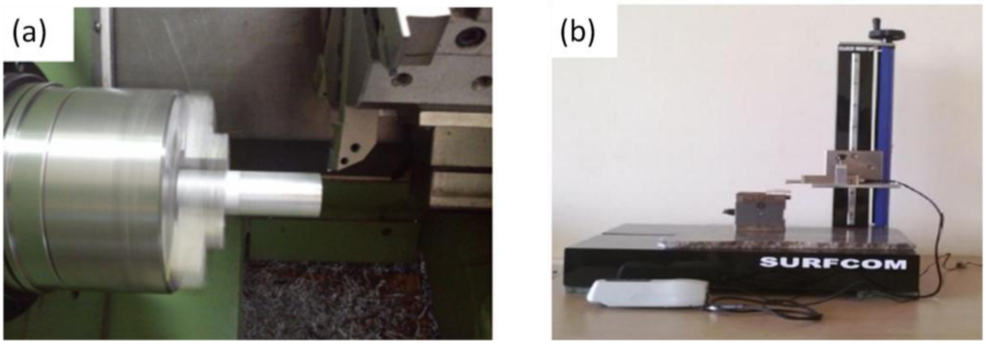

Figure 2. (a) Sample mounted in Smart Jr CNC turning centre; (b) Handysurf surface roughness measuring device.

3. Results and discussions

3.1. Microstructures of AA 7075/TiC AMCs

The optical microscope images of the manufactured AA 7075 reinforced with 0, 2.5, 5 and 7.5 wt% TiC particles are shown in Figure 3a,b,c,d respectively. Some shrinkages and or slag inclusion had also observed which was usually occurring in the casting process. From Figure 3, it was clearly noted that the uniform distribution of TiC ceramic particles over the matrix had occurred up to 5 wt% TiC and then the observed size of TiC particles had shown large size which had expected to agglomeration. The formation of clustering with the incorporation of fine reinforcement particles over the matrix had also reported by several researchers [28–31]. The tendency to cluster formation in fine reinforcements had expected to the Vander Waal’s force of attraction among the ceramic particles [32–35], large variation in cooling velocity inside the sample during solidification, and large differences in thermal conductivity between the matrix and the reinforcement. In fact, as the percentage of fine TiC ceramic particles had incorporated in the melt subsequently the viscosity of melt had expected to low due to which the TiC particle clustering had expected to start [35]. Further, the observed uniform distribution of TiC particles had ensured the good wettability occurred between the α-Al matrix and TiC ceramic particles [29]. The interface bonding between the fine TiC particles with the matrix had checked by conducting the scanning electron microscopy with EDS for AA 7075–5 wt% TiC sample as an example which is shown in Figure 4. From Figure 4a, the TiC particles had completely embedded with the AA 7075 matrix alloy which confirmed the proper interface between the matrix and reinforcement. Figure 4b shows the EDAX spectrum which confirmed the presence of α-Al matrix and TiC particles.

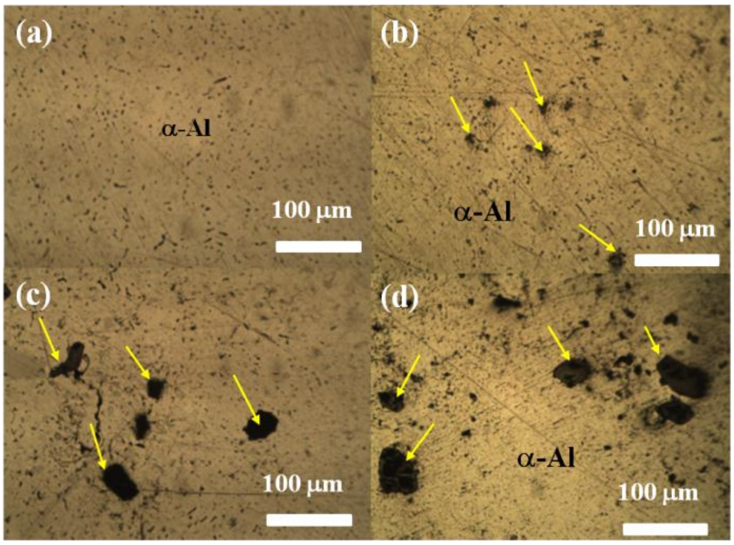

Figure 3. Microstructural images of (a) AA 7075–0 wt% TiC; (b) AA 7075–2.5 wt% TiC; (c) AA 7075–5 wt% TiC; (b) AA 7075–7.5 wt% TiC.

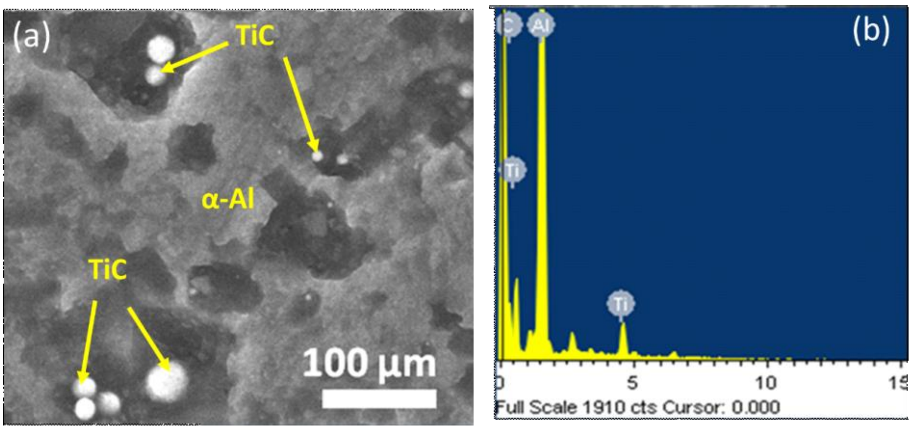

Figure 4. (a) SEM microstructure of AA 7075–5 wt% TiC composite; (b) EDS on (a).

3.2. Mechanical behavior of AA 7075/TiC AMCs

The mechanical behavior of the fabricated AA 7075 reinforced with the different weight percentage of TiC particles composites had performed by Rockwell hardness test. Table 2 had illustrated the variation of hardness strength with the function of TiC particles in the AA 7075 matrix. The results had explained clearly that the strength of the matrix had started to increases with the function of TiC particles in the matrix. The average Rockwell hardness value of fabricated composites had around 110 HRC, 134 HRC, 172 HRC, and 218 HRC for 0, 2.5, 5, and 7.5 wt% TiC reinforced composites. These results had revealed that the strength of the AA 7075 matrix had increased with the function of second phase particles of TiC which had attributed to Orowan strengthening mechanism. The highly reinforced AA 7075/7.5 wt% TiC composite had exhibited the strength of around two times more than the unreinforced AA 7075 matrix. These results had clearly explained that the strength of the composites could be improved by incorporating the TiC particles in the AA 7075 matrix.

Table 2. Rockwell hardness of AA 7075/(0, 2.5, 5 & 7.5 wt%) TiC composites.

S. No.	Materials	Rockwell hardness, HRC
01	AA 7075–0 wt% TiC	110 ± 5.5
02	AA 7075–2.5 wt% TiC	134 ± 3.8
03	AA 7075–5 wt% TiC	172 ± 4.2
04	AA 7075–7.5 wt% TiC	218 ± 3.6

3.3. Turning behavior of AA 7075/TiC AMCs

The turning behavior had carried out on monolithic AA 7075 alloy and AA 7075–7.5 wt% TiC composites (higher reinforced sample) as an example. The values of surface roughness at different cutting speeds, feed rates, and depth of cuts while turning of unreinforced Al alloy and AA 7075 + 7.5 wt% TiC composites using carbide insert with 0.4 mm and 0.8 mm nose radius are shown in Table 3 and Figure 5. Figure 5 had drawn in the same scale with the function of input parameters. From Figure 5, it was clear that the value of surface roughness had started to increases drastically with the function of both the feed rate and depth of cut in all the samples. However, the sample of AA 7075 + 7.5 wt% TiC composite machined using 0.8 mm nose radius had produced a lower value of surface roughness. In both the alloy and composites, the surface roughness value had decreased considerably when the insert tool nose radius had increased from 0.4 to 0.8 mm. These results had indicated that the composites had exhibited improved surface finish when compared to the monolithic alloy. This result had expected to higher strength in the composites which might have produced immediate shearing action. Further, the improved value of surface roughness with the function of tool nose radius had attributed to more contact which had occurred in between the tool and the workpiece for the higher value of insert tool nose radius. Due to a lower amount of contact between the tool and the workpiece for 0.4 mm nose radius tool, it had produced more value of surface roughness [35]. For instance, the SEM surface morphology of AA 7075–7.5 wt% TiC after turning at the highest and lowest cutting parameters of 0.8 mm turned samples had taken which is shown in Figure 6. The results had clearly explained that there was no feed marks, pit holes, tiny marks (Figure 6a) at the highest cutting speed with lowest feed rate and depth of cut. However, there were more feed marks, pit holes, and tiny marks (Figure 6b) at the lowest cutting speed with highest feed rate and depth of cut. These results had demonstrated that the surface roughness had mainly depended on the cutting speed. The decreasing of surface roughness with increasing of cutting speed had observed, investigated, and discussed by Kaya et al. [36] while turning of AA 7075 alloy. The authors had reported that the surface roughness value had varied with cutting speed and different heat treatment condition. For comparison, in AA 7075 alloy at 220 m/min cutting speed, the same authors had reported the surface roughness value of 4.4 µm whereas the maximum of 4 µm (0.4 mm nose radius) and 2.28 µm (0.8 mm nose radius) had observed in the present work. This result had revealed that the present work and the Kaya et al. [36] had matched exactly. Therefore, the surface finish and tool life would be improved when we use 0.8 mm insert tool radius.

Table 3. Experimental values of surface roughness by using 0.4 mm and 0.8 mm nose radius.

Materials	Feed (mm/rev)	Depth of cut (mm)	Cutting speed (m/min)	Average surface roughness (µm)	
				0.4 mm nose radius insert	0.8 mm nose radius insert
AA 7075 alloy (unreinforced alloy)	0.1	0.5	180	0.959	0.671
			200	0.888	0.532
			220	0.578	0.355
			240	0.412	0.264
	0.2	1.0	180	2.89	1.662
			200	2.69	1.512
			220	2.34	1.458
			240	2.12	1.241
	0.3	1.5	180	4.642	2.648
			200	4.472	2.556
			220	3.994	2.208
			240	3.558	1.95
AA 7075–7.5 wt% TiC	0.1	0.5	180	0.872	0.607
			200	0.863	0.559
			220	0.766	0.456
			240	0.697	0.416
	0.2	1.0	180	2.654	1.240
			200	1.982	1.211
			220	1.877	1.161
			240	1.736	1.011
	0.3	1.5	180	3.775	2.809
			200	3.675	2.572
			220	3.205	2.473
			240	2.911	2.112

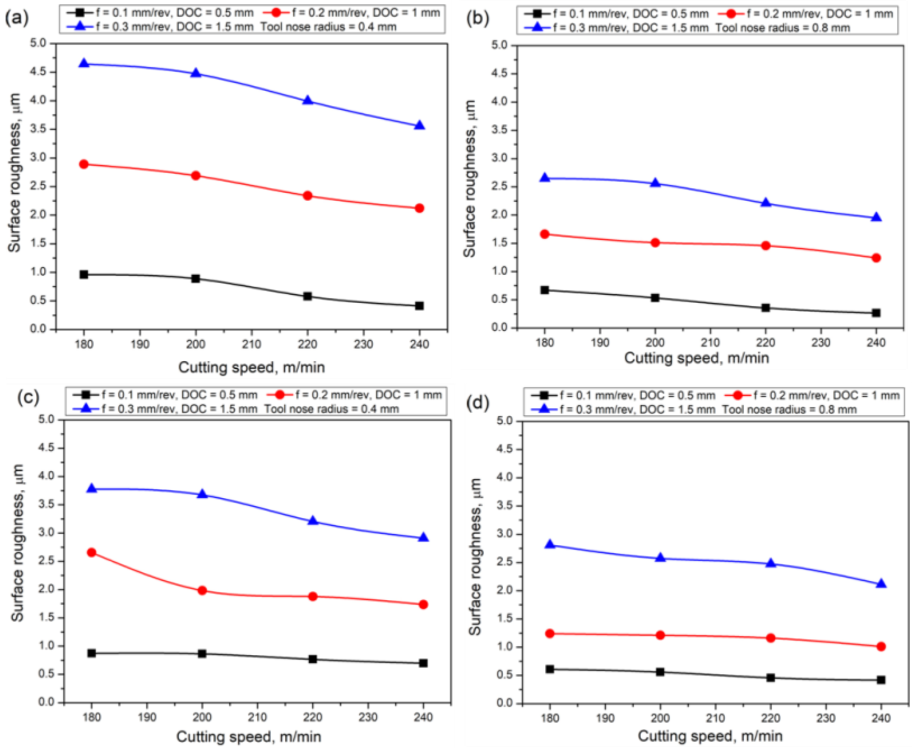

Figure 5. Variations of surface roughness of (a) AA 7075 + 0 wt% TiC (0.4 mm nose radius); (b) AA 7075 + 0 wt% TiC (0.8 mm nose radius); (c) AA 7075 + 7.5 wt% TiC composites (0.4 mm nose radius); (d) AA 7075 + 7.5 wt% TiC composites (0.8 mm nose radius).

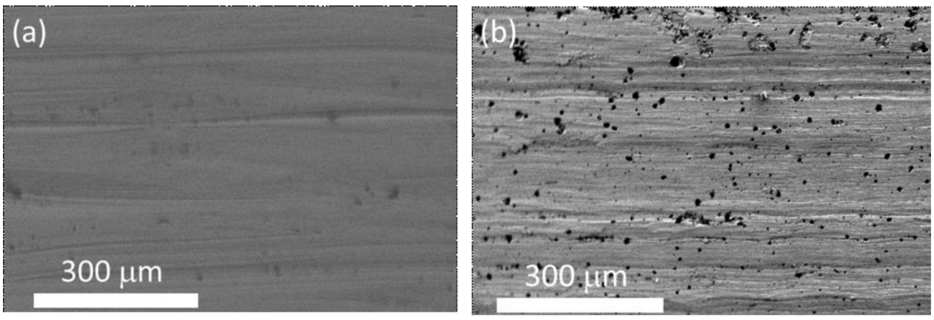

Figure 6. SEM images on turned surface (0.8 mm nose radius): (a) AA 7075–7.5 wt% TiC, at 240 m/min cutting speed, 0.1 mm/rev feed rate, and 0.5 mm depth of cut; (b) AA 7075–7.5 wt% TiC, at 180 m/min cutting speed, 0.3 mm/rev, and 1.5 mm depth of cut.

Figure 7 shows the chip morphology of Al 7075 monolithic alloy and AA 7075–7.5 wt% TiC composites turned by using coated carbide tool of nose radius of 0.8 mm. A very thin almost continuous chip had observed in TiC reinforced alloy. The lower amount of continuous chips and discontinuous chip had observed in as-cast unreinforced Al 7075 alloy. Further, for the low feed rate, low depth of cut and high cutting speed, less serration had observed in the case of reinforced composite (Figure 7d,h). A very fine chip thickness had observed in AA 7075–7.5 wt% TiC composites whereas a very coarse and high serration chips had obtained in AA 7075 monolithic alloy. Based on the results, 0.8 mm nose radius insert tool had exhibited good surface finish irrespective of composition and cutting parameters.

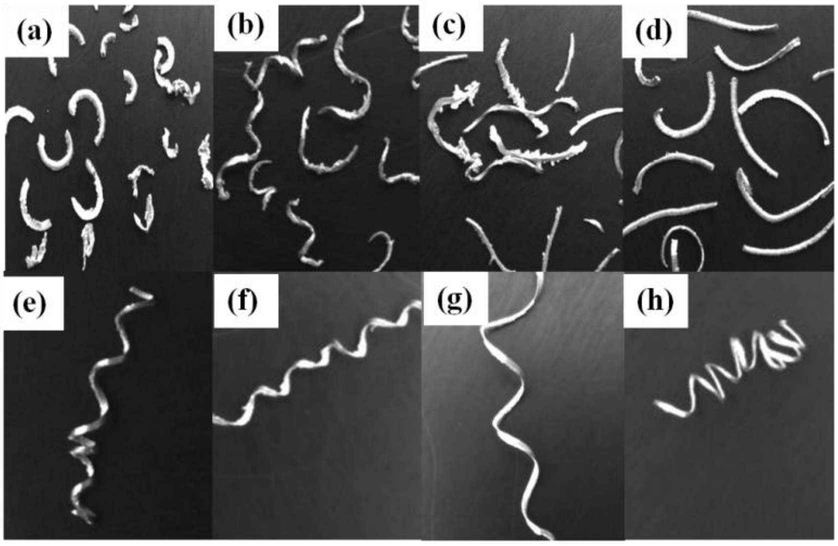

Figure 7. Variation of chip morphology with the function of cutting speed (f = 0.1 mm/rev, DOC = 0.5 mm, 0.8 mm nose radius): (a–d) AA 7075 + 0 wt% TiC; (e–h) AA 7075 + 7.5 wt% TiC composites.

4. Conclusions

The influence of TiC particles addition to the Al 7075 alloy, the microstructural characterizations, and the surface roughness variation during the turning had investigated and reported. Based on the results, the following conclusions had drawn from this study:

- Altered TiC wt% of reinforcement particles were successfully incorporated into the matrix through stir casting technique.
- Consecutively, the produced composites had the uniform distribution of second phase particles (TiC) in the Al alloy upto 5 wt% TiC reinforced composite. However, beyond 5 wt% TiC, agglomeration of TiC particles had observed due to Vander Waals force of attraction.
- The proper interface between the TiC particles with the AA 7075 matrix had achieved which had evidenced through SEM with EDS.
- The highly reinforced AA 7075/7.5 wt% TiC composite had exhibited the strength of around two times more than the unreinforced AA 7075 matrix.
- The increasing of reinforcement in the matrix had exhibited improved surface finish due to increase in strength in the matrix, dispersion strengthening, and effective bonding.

Acknowledgments

The corresponding author wishes to thank the Qassim University for all funding and support required to carry out this research.

Conflicts of interest

The author declares no conflict of interest.

References

1. Guo RF, Shen P, Sun C, et al. (2016) Processing and mechanical properties of lamellar-structured Al–7Si–5Cu/TiC composites. *Mater Design* 106: 446–453.
2. Melgarejo ZH, Suarez OM, Sridharan K (2006) Wear resistance of a functionally-graded aluminum matrix composite. *Scripta Mater* 55: 95–98.
3. Vieira AC, Sequeira PD, Gomes JR, et al. (2009) Dry sliding wear of Al alloy/SiC_p functionally graded composites: influence of processing conditions. *Wear* 267: 585–592.
4. Rodrıguez-Castro R, Wetherhold RC, Kelestemur MH (2002) Microstructure and mechanical behavior of functionally graded Al A359/SiC_p composite. *Mater Sci Eng A-Struct* 323: 445–456.
5. Prabhu TR (2015) Effects of solid lubricants, load, and sliding speed on the tribological behavior of silica reinforced composites using design of experiments. *Mater Design* 77: 149–160.
6. Uyyuru RK, Surappa MK, Brusethaug S (2006) Effect of reinforcement volume fraction and size distribution on the tribological behavior of Al-composite/brake pad tribo-couple. *Wear* 260: 1248–1255.
7. Lin QL, Shen P, Yang LL, et al. (2011) Wetting of TiC by molten Al at 1123–1323 K. *Acta Mater* 59: 1898–1911.
8. Rana RS, Purohit R, Das S (2012) Review of recent studies in Al matrix composites. *Int J Sci Eng Res* 3: 1–16.
9. Li P, Kandalova EG, Nikitin VI (2005) In situ synthesis of Al–TiC in aluminum melt. *Mater Lett* 59: 2545–2548.
10. Shaga A, Shen P, Sun C, et al. (2015) Lamellar-interpenetrated Al–Si–Mg/SiC composites fabricated by freeze casting and pressureless infiltration. *Mater Sci Eng A-Struct* 630: 78–84.
11. Deuis RL, Subramanian C, Yellup JM (1997) Dry sliding wear of aluminium composites—a review. *Compos Sci Technol* 57: 415–435.
12. Mazahery A, Shabani MO (2012) Study on microstructure and abrasive wear behavior of sintered Al matrix composites. *Ceram Int* 38: 4263–4269.
13. Kennedy AR, Weston DP, Jones MI (2001) Reaction in Al–TiC metal matrix composites. *Mater Sci Eng A-Struct* 316: 32–38.
14. Vieira AC, Sequeira PD, Gomes JR, et al. (2009) Dry sliding wear of Al alloy/SiC_p functionally graded composites: influence of processing conditions. *Wear* 267: 585–592.
15. Rajan TPD, Pillai RM, Pai BC (2010) Characterization of centrifugal cast functionally graded aluminum-silicon carbide metal matrix composites. *Mater Charact* 61: 923–928.
16. Melgarejo ZH, Suarez OM, Sridharan K (2008) Microstructure and properties of functionally graded Al–Mg–B composites fabricated by centrifugal casting. *Compos Part A-Appl S* 39: 1150–1158.
17. Lu HX, Hu J, Chen CP, et al. (2005) Characterization of Al_2O_3–Al nano-composite powder prepared by a wet chemical method. *Ceram Int* 31: 481–485.

18. Yang DL, Qiu F, Zhao QL, et al. (2017) The microstructure and tensile property for Al2014 composites reinforced with Ti_5Si_3-coated SiC_P. *Mater Sci Eng A-Struct* 688: 459–463.
19. Kim CS, Cho K, Manjili MH, et al. (2017) Mechanical performance of particulate-reinforced Al metal-matrix composites (MMCs) and Al metal-matrix nano-composites (MMNCs). *J Mater Sci* 52: 13319–13349.
20. Baradeswaran A, Perumal AE (2013) Influence of B_4C on the tribological and mechanical properties of Al 7075–B_4C composites. *Compos Part B-Eng* 54: 146–152.
21. Geng J, Hong T, Ma Y, et al. (2016) The solution treatment of *in-situ* sub-micron TiB_2/2024 Al composite. *Mater Design* 98: 186–193.
22. Evans A, San Marchi C, Mortensen A (2003) Processing Metal Matrix Composites, In: Evans A, San Marchi C, Mortensen A, *Metal Matrix Composites in Industry*, Springer, Boston, MA, 39–64.
23. Sivasankaran S, Harisagar PT, Saminathan E, et al. (2014) Effect of nose radius and graphite addition on turning of AA 7075-ZrB_2 in-situ composites. *Procedia Eng* 97: 582–589.
24. Ramkumar KR, Bekele H, Sivasankaran S (2015) Experimental investigation on mechanical and turning behavior of Al 7075/x% wt. TiB_2-1% Gr in-situ hybrid composite. *Adv Mater Sci Eng* 2015: 727141
25. Palainasamy A, Selvaraj T, Sivasankaran S (2017) Taguchi-based grey relational analysis for modeling and optimizing machining parameters through dry turning of Incoloy 800H. *J Mech Sci Technol* 31: 4159–4165.
26. Teague EC, Vorburger TV, Maystre D, et al. (1981) Light scattering from manufactured surfaces. *CIRP Ann-Manuf Techn* 30: 563–569.
27. Li L, Collins SA, Yi AY (2010) Optical effects of surface finish by ultra precision single point diamond machining. *ASME J Manuf Sci Eng* 132: 021002.
28. Wang Y, Shen P, Guo RF, et al. (2017) Developing high toughness and strength Al/TiC composites using ice-templating and pressure infiltration. *Ceram Int* 43: 3831–3838.
29. Mohapatra S, Chaubey AK, Mishra DK, et al. (2016) Fabrication of Al–TiC composites by hot consolidation technique: its microstructure and mechanical properties. *J Mater Res Technol* 5: 117–122
30. Sivasankaran S, Sivaprasad K, Narayanasamy R, et al. (2010) An investigation on flowability and compressibility of AA 6061_{100-x}-x wt.% TiO_2 micro and nanocomposite powder prepared by blending and mechanical alloying. *Powder Technol* 201: 70–82.
31. Ramkumar KR, Sivasankaran S, Alaboodi AS (2017) Effect of alumina content on microstructures, mechanical, wear and machining behavior of Cu-10Zn nanocomposite prepared by mechanical alloying and hot-pressing. *J Alloy Compd* 709: 129–141.
32. Gawdzińska K, Chybowski L, Przetakiewicz W (2016) Proper matrix-reinforcement bonding in cast metal matrix composites as a factor of their good quality. *Arch Civ Mech Eng* 16: 553–563.
33. Basak AK, Pramanik A, Islam MN, et al. (2015) Challenges and recent developments on nanoparticle-reinforced metal matrix composites, In: Dong Y, Umer R, Lau AKT, *Fillers and Reinforcements for Advanced Nanocomposites*, A volume in Woodhead Publishing Series in Composites Science and Engineering, 349–367.
34. Prabhu TR (2017) Processing and properties evaluation of functionally continuous graded 7075 Al alloy/SiC composites. *Arch Civ Mech Eng* 17: 20–31.

35. Savas O, Kayicki R, Ficici F, et al. (2014) Production of functionally graded SiC/Al-Cu-Mg composite by centrifugal casting. *Sci Eng Compos Mater* 21: 1–5.
36. Kaya H, Uçar M, Cengiz A, et al. (2012) The effect of aging on the machinability of AA7075 aluminium alloy. *Sci Res Essays* 7: 2424–2430.

AIMS Press

© 2018 the Author(s), licensee AIMS Press. This is an open access article distributed under the terms of the Creative Commons Attribution License (http://creativecommons.org/licenses/by/4.0)